

Neutrino-nucleus reactions in the delta resonance region

B. Szczerbinska^{a,c} T. Sato^b K. Kubodera^c T. -S. H. Lee^d

^a*Dakota State University, Madison, South Dakota 57020, USA*

^b*Department of Physics, Osaka University, Toyonaka, Osaka 560-0043, Japan*

^c*Department of Physics and Astronomy, University of South Carolina, Columbia, South Carolina 29208, USA*

^d*Physics Division, Argonne National Laboratory, Argonne, Illinois 60439, USA*

Abstract

Reliable estimates of neutrino-nucleus reactions in the resonance-excitation region play an important role in many of the on-going and planned neutrino oscillation experiments. We study here neutrino-nucleus reactions in the delta-particle excitation region with the use of neutrino pion-production amplitudes calculated in a formalism in which the resonance contributions and the background amplitudes are treated on the same footing. Our approach leads to the neutrino-nucleus reaction cross sections that are significantly different from those obtained in the conventional approach wherein only the pure resonance amplitudes are taken into account. To assess the reliability of our formalism, we calculate the electron-nucleus scattering cross sections in the same theoretical framework; the calculated cross sections agree reasonably well with the existing data.

Key words:

PACS: 13.15.+g, 13.60.Le, 25.30.Rw, 25.30.Pt

1 Introduction

It is well recognized that the precise knowledge of neutrino-nucleus reaction cross sections is of importance in analyzing neutrino oscillation experiments; for recent reports, see *e.g.* Refs. [1,2,3,4,5]. In particular, neutrino-nucleus reactions at incident neutrino energies around 1 GeV play a prominent role in many cases including the experiments at K2K [2]. To obtain estimates of the relevant cross sections, one must at present rely on theory, and much theoretical effort has been invested to provide these estimates [6,7,8,9,10,11].

In an attempt to make a quantitative estimation of neutrino-nucleus reaction cross sections, it is useful to study simultaneously the related electron-nucleus reactions within the same general theoretical framework, and this strategy has been pursued by many authors. In electron-nucleus scattering in the GeV region, quasi-elastic scattering and pion-production processes are known to be the main reaction mechanisms, and similar features are expected to manifest themselves also in the neutrino-nucleus reactions in the GeV region.

For quasi-elastic scattering, the relevant transition operators are essentially known, so the main theoretical issue is how to incorporate various nuclear effects for the initial and final states. The early works were based on the Fermi gas model [12,13], but recent investigations incorporate the nuclear correlation effects in the initial state with the use of the spectral function and take account of the final-state interactions on the outgoing nucleon [7]. As regards the pion-production process, in addition to these nuclear effects, the structure of the transition operators responsible for pion production needs to be carefully studied. These operators can in principle involve more than one nucleon, but it is in general expected that pion production on a single nucleon should give a dominant contribution. Neutrino-induced pion production on the nucleon in the resonance region has been studied so far mostly with the use of pure resonance excitation amplitudes. In some studies these amplitudes were evaluated in the quark model, see, e.g., Ref. [14]. In recent studies by Paschos and his collaborators [15,16], the resonance excitation amplitudes due to the vector current were directly related to the empirically known electro-excitation amplitudes, while those due to the axial-vector current were constrained by invoking PCAC.

Meanwhile, it is to be noted that pion production can take place not only through resonance excitations but also via non-resonant processes. Two of the present authors [17,18] have recently developed a dynamical model for describing photo- and electro-production of pions off the nucleon around the Δ -resonance region, with the view to systematically incorporating both the resonance and non-resonance contributions. Hereafter we refer to this approach as the SL-model (the Sato-Lee model). The development of the SL-model was motivated by recent extensive experimental studies of electron- and photon-induced meson-production reactions on the nucleon in the resonance region. The main objective of these experiments is to study the non-perturbative features of QCD by testing the resonance properties as predicted by QCD-inspired models and/or lattice simulations. The SL-model was subsequently extended to weak-interaction processes [19,20], and it was shown that this model gives a successful description of neutrino-induced pion production in the Δ -resonance region.

As explained in more detail later, the SL-model starts from the non-resonant meson-baryon interaction and the resonance interaction, and the unitary am-

plitudes are obtained from the scattering equation. It leads to fairly consistent descriptions of all the available data for the electroweak reactions in the Δ -resonance region. It has been shown that treating the resonance and non-resonance amplitudes on the same footing can have significant observable consequences. In particular, the inclusion of the pion cloud effects as considered in SL can resolve a long-standing puzzle that the N - Δ magnetic dipole transition form factor G_M predicted by the quark model is smaller than the empirical value by as much as $\sim 40\%$. Furthermore, the electric $E2(G_E)$ and Coulomb $C2(G_C)$ form factors for the N - Δ transition in electron scattering calculated in the SL-model show pronounced momentum dependences due to the pion cloud effects, which suggests non-negligible deformation effects in the N - Δ transition. Regarding the neutrino reactions, a serious problem that has been known for quite some time is that the axial-vector N - Δ transition strength calculated in the constituent quark model [21] is lower than the empirical value [22] by about 35 %. It is noteworthy that the dynamical pion cloud effects included in the SL-model [19] can naturally remove this discrepancy.

In view of these successes, it seems worthwhile to study neutrino-nucleus reactions in the resonance region with the use of the SL-model amplitudes for neutrino-induced pion production on the nucleon. We describe here our first attempt at such a study and present the cross sections, the energy spectrum of the final lepton (for charged-current reactions), and the lepton-momentum transfer distribution. Our work is basically of exploratory nature and, as far as the nuclear effects are concerned, we only consider those that can be taken into account with the use of a modified Fermi gas model wherein nuclear correlations are approximately subsumed into the spectral function [7]. Despite these limitations, our investigation is hoped to be informative as the first calculation of neutrino-nucleus reactions in the Δ -resonance region based on the electroweak pion-production amplitudes calculated in SL [17,18], whose validity has been extensively tested by the Jlab data [23,24]. It is understood that, as the experimental precision improves, more detailed calculations will be called for that incorporate higher order effects. In particular, the final-state interaction (FSI) must be treated properly. As discussed in Ref. [7] and many earlier works on inclusive electron scattering, FSI re-distributes the inclusive cross sections and, for the incident electron energy around 1 GeV, FSI can reduce the strength at the quasi-free peak by about 10 %. We remark that a detailed study [25] indicates that the FSI effects for inclusive reactions, properly treated, can be rather different from those for exclusive processes [26]. Meanwhile, in the pion production region, we need to take into account pion absorption and medium effects on Δ propagation. To this end, one may profitably use the information obtained in the well-developed Δ -hole model [27]; such a study has been made in Ref. [28] within the framework of the dynamical transport approach. Our present calculation, however, falls short of considering FSI. Since the importance of these FSI effects grows rather fast with the increasing target mass number (this is particularly true for pion absorption),

we limit ourselves here to nuclear targets of low mass numbers and concentrate on the $A=12$ target. Although heavier nuclei such as ^{56}Fe are important in some neutrino-oscillation experiments [5], we can deal with these cases only after FSI is incorporated into our formalism.

2 Sato-Lee (SL) Model

As the SL-model has been fully described in Refs. [17,18,19,20], we give here only a brief explanation of the model, using as an example the case of pion photoproduction. The effective Hamiltonian H_{eff} in the SL-model for this process is given by

$$H_{eff} = H_0 + v_{\pi N} + v_{\gamma\pi} + \Gamma_{\pi N \leftrightarrow \Delta} + \Gamma_{\gamma N \leftrightarrow \Delta}, \quad (1)$$

where H_0 is the free Hamiltonian; $v_{\pi N}$ and $v_{\gamma\pi}$ represent the non-resonant pion-nucleon and pion photoproduction interactions, respectively, while $\Gamma_{\pi N \leftrightarrow \Delta}$ and $\Gamma_{\gamma N \leftrightarrow \Delta}$ are responsible for the creation and annihilation of a bare Δ -resonance. By solving the Lippmann-Schwinger equation based on the above effective Hamiltonian, we obtain the amplitude for pion production on a nucleon as

$$T_{\gamma\pi} = t_{\gamma\pi}(E) + \frac{\bar{\Gamma}_{\Delta \rightarrow \pi N}(E)\bar{\Gamma}_{\gamma N \rightarrow \Delta}(E)}{E - m_{\Delta}^0 - \Sigma(E)}, \quad (2)$$

where E is the total energy of the pion and nucleon in the center-of-mass system. The first term $t_{\gamma\pi}$ is the non-resonant amplitude, which arises from the vertices $v_{\pi N}$ and $v_{\gamma N}$ alone, while the second term represents the resonant amplitude involving the dressed vertex $\bar{\Gamma}$. We note that the bare resonance vertex Γ is renormalized into $\bar{\Gamma}$ by the non-resonant meson cloud effects arising from rescattering as

$$\bar{\Gamma}_{\gamma N \rightarrow \Delta}(E) = \Gamma_{\gamma N \rightarrow \Delta} + \Gamma_{\pi N \rightarrow \Delta} G_0 t_{\gamma\pi}(E), \quad (3)$$

and that the renormalized resonance vertex $\bar{\Gamma}$ should exhibit a significant deviation from the bare vertex Γ because of the meson cloud effects. In conventional analyses, however, one disregards the difference between the bare and renormalized resonance vertices and, assuming the Breit-Wigner form for (what in our approach is identified as) the renormalized vertex, tries to extract the parameters characterizing that form by fitting to the data. However, as discussed in detail in Refs. [17,18,19,20] and as briefly mentioned in the introduction, the resonance properties deduced from this simplified treatment tend to exhibit significant discrepancies with the theoretical predictions, indicating

the importance of considering the resonant and non-resonant contributions simultaneously.

We expect that the unified treatment of the resonant and non-resonant contributions should have significant consequences in the neutrino-nucleon and neutrino-nucleus reactions as well. To illustrate this point, we give in Fig. 1 the electron energy spectrum $d\sigma/dE_e$ for the $\nu_e N \rightarrow e^- \pi N$ reaction calculated in the SL-model. Since the isospin of the πN system for the $\nu_e p \rightarrow e^- \pi^+ p$ reaction is $3/2$, one may naively expect that the Δ -resonance amplitude dominates the cross section. However, the energy spectra obtained in our SL-model calculation (shown in the solid lines) are markedly different from those obtained from the dressed resonant amplitudes (shown in the long-dash lines). For comparison, the results obtained in the Lalakulich-Paschos (LP) model [15] are also shown in the short dashed lines. If in our approach we drop the contribution of the non-resonant amplitudes (retaining only the resonance contributions), the results turn out to be very similar to those obtained in the LP-model.

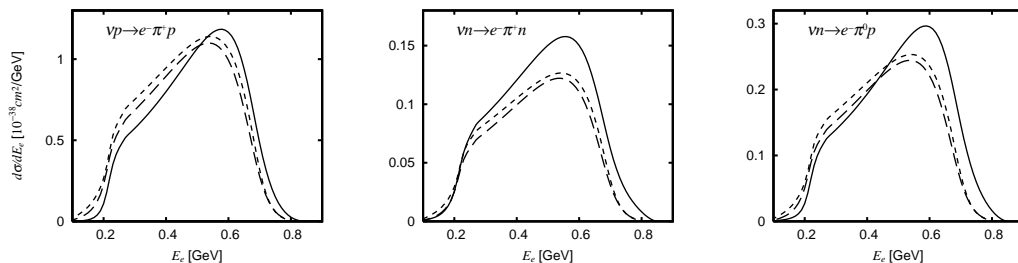


Fig. 1. Electron energy spectrum for $\nu_e p \rightarrow e^- \pi^+ p$ (left panel), $\nu_e n \rightarrow e^- \pi^+ n$ (middle panel), and $\nu_e n \rightarrow e^- \pi^0 p$ (right panel). For the explanation of the three curves in each panel, see the text.

Since neutrino-nucleus reactions obviously involve both νp and νn reactions, it is also informative to examine how the non-resonant contributions can affect the relative importance of the νp and νn contributions. If the $I = 3/2$ resonance amplitude dominates, the cross section on the neutron should be $1/3$ of that for the proton. Fig. 2 shows $d\sigma/dQ^2$ for the proton target (solid line) and $3 \times d\sigma/dQ^2$ for the neutron target (long-dashed line) for $E_\nu = 1$ GeV. The curves should agree with each other if the delta mechanism dominates. However, the neutron cross section is about 20% larger than the value expected from Δ dominance. The short-dashed line gives $d\sigma/dQ^2$ for the proton target obtained with the use of the dressed resonance amplitude alone. We note that this curve overlaps rather well with the solid line corresponding to the SL-model results, a feature to be contrasted with the behavior of $d\sigma/dE_e$ shown in Fig. 1. We learn from this that, even for the same reaction, some observables are more sensitive than others to the difference between the SL-model results and those of the resonance-contribution-only approach.

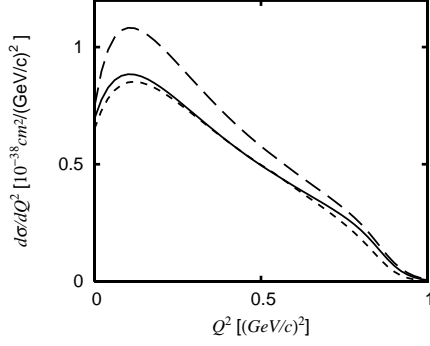


Fig. 2. Differential cross sections $d\sigma/dQ^2$ for $\nu_e N \rightarrow e^- \pi N$ at $E_\nu = 1$ GeV, where $Q^2 = -q^2$ and $q \equiv p_e - p_\nu$ is the lepton momentum transfer. Solid line – proton target (SL-model calculation); short-dashed line – proton target (resonance amplitude only); long-dashed line – neutron target case multiplied with a factor of 3 (SL-model calculation). The final πN state is $\pi^+ p$ for the proton target, whereas both $\pi^0 p$ and $\pi^+ n$ can contribute in the neutron target case.

3 Neutrino-nucleus reaction

We consider the charged-current (CC) neutrino-nucleus reaction

$$\nu_\ell(p_\nu) + |i(P_i)\rangle \rightarrow \ell(p_\ell) + |f(P_f)\rangle, \quad (4)$$

where $|i\rangle$ represents a target nucleus of mass A , $|f\rangle$ stands for a final hadronic state, and ℓ is a lepton flavor ($\ell = e, \mu, \tau$); the relevant momenta are indicated in the parentheses. The cross section for this process is given in terms of the lepton tensor $L_{\mu\nu}$ and the hadron tensor $W^{\mu\nu}$ as

$$\frac{d\sigma}{dE_\ell d\Omega_\ell} = \frac{p_\ell}{p_\nu} \frac{G_F^2 \cos^2 \theta_c}{8\pi^2} L_{\mu\nu} W^{\mu\nu}. \quad (5)$$

The lepton tensor is expressed as

$$L^{\mu\nu} = 2 [p_\ell^\mu p_\nu^\nu + p_\ell^\nu p_\nu^\mu - g^{\mu\nu} (p_\nu \cdot p_\ell - m_\ell^2) + i\epsilon^{\mu\nu\alpha\beta} p_{\nu,\alpha} p_{\ell,\beta}], \quad (6)$$

where m_ℓ is the mass of the final lepton. The hadron tensor is related to the matrix elements of the hadronic weak current J^μ as

$$W^{\mu\nu} = \sum_i \sum_f (2\pi)^3 V \delta^4(P_f + p_\ell - P_i - p_\nu) \langle f | J^\mu | i \rangle \langle f | J^\nu | i \rangle^*,$$

where V is the quantization volume. In the Fermi-gas model, $W^{\mu\nu}$ can be related to the single-nucleon transition amplitudes, and the relation for the case of quasi-elastic scattering is well known [12]. For a single-pion production process, $W^{\mu\nu}$ is given as

$$\begin{aligned}
W^{\mu\nu} &= \int d\vec{p}' d\vec{k} d\vec{p} \theta(p_F - |\vec{p}'|) \theta(|\vec{p}'| - p_F) \delta^4(p + q - p' - k) \\
&\times \frac{1}{(2\pi)^3} \frac{m_N^2}{E_N(p) E_N(p') 2E_\pi(k)} \frac{3}{4\pi p_F^3} \\
&\times \sum_{s_N, s_{N'}, i, t_N} \frac{N_{t_N}}{2} \langle \pi^i N(p', s_{N'}, t_{N'}) | j^\mu | N(p, s_N, t_N) \rangle \\
&\quad \times \langle \pi^i N(p', s_{N'}, t_{N'}) | j^\nu | N(p, s_N, t_N) \rangle^*
\end{aligned} \tag{7}$$

Here p (p') is the four-momentum of the initial (final) nucleon, k is the four-momentum of the pion, $q = p_\nu - p_l$, and p_F is the Fermi momentum; $N_{t_N} = Z/N$ are the proton and neutron numbers in the target nucleus; s_N and t_N are the spin and isospin of the struck nucleon, while i is the isospin index of the pion. The matrix element of the nucleon current for pion production, $\langle \pi^i N(p', s_{N'}, t_{N'}) | j^\mu | N(p, s_N, t_N) \rangle$, is calculated using the SL model. Since SL gives the pion-production amplitude in the pion-nucleon center-of-mass frame (πN -cm frame, for short), we transform it into the amplitude in the rest frame of the target nucleus (LAB frame) according to

$$\begin{aligned}
W^{\mu\nu} &= \sum_{s_N, s_{N'}, t_N, i} \frac{3}{4\pi p_F^3} \int d\vec{p}' \theta(p_F - |\vec{p}'|) \frac{m_N}{E_N(p)} \\
&\times N_{t_N} \int d\Omega_* \theta(|\vec{p}'| - p_F) \frac{|\vec{k}_c| m_N}{32\pi^2 W} \\
&\times \Lambda^{\mu\mu'} \langle \pi^i N(p', s_{N'}) | j^{\mu'} | N(p, s_N, t_N) \rangle_{\pi N\text{-cm}} \\
&\times \Lambda^{\nu\nu'} \langle \pi^i N(p', s_{N'}) | j^{\nu'} | N(p, s_N, t_N) \rangle_{\pi N\text{-cm}}^*,
\end{aligned} \tag{8}$$

where W is the invariant mass of the pion and nucleon given by $W = \sqrt{(p' + k)^2}$. The Lorentz transformation matrix $\Lambda^{\mu\nu}$ transforms vectors in the πN -cm frame to those in the LAB frame. In the πN -cm frame, $p' + k = (W, \vec{0})$, whereas in the LAB frame we identify $p' + k = p + q = (\sqrt{\vec{p}^2 + m_N^2} - B + \omega, \vec{p} + \vec{q})$; thus the nuclear binding correction is taken into account with the use of $p^\mu = (\sqrt{\vec{p}^2 + m_N^2} - B, \vec{p})$. We note that the Pauli blocking factor, $\theta(|\vec{p}'| - p_F)$, is dependent on the pion momentum \vec{k} through $\vec{p}' = \vec{p} + \vec{q} - \vec{k}$, and hence the consideration of the Pauli blocking effect requires the knowledge of the pion-production amplitude. We come back to this point later.

We take into account the nuclear correlation effects in the initial state by using the spectral function $P(\vec{p}, E)$ obtained in Ref. [29]. This is achieved by

the following replacements in Eq. (8)

$$\frac{3}{4\pi p_F^3} \int d\vec{p} \theta(p_F - |\vec{p}|) \rightarrow \int d\vec{p} dEP(\vec{p}, E) \quad (9)$$

$$p^0 = \sqrt{\vec{p}^2 + m_N^2} - B \rightarrow m_N - E. \quad (10)$$

We note that $P(\vec{p}, E)$ is normalized as $\int d\vec{p} dEP(\vec{p}, E) = 1$. Although the use of the spectral function implies that the separation of occupied and empty nucleon orbits based on the Fermi momentum p_F is no longer strictly valid, we choose to retain the factor $\theta(|\vec{p}| - p_F)$ in Eq.(8) to approximately take account of Pauli blocking for the final nucleon.

4 Results and Discussion

Using the formalism explained in the previous section, we calculate neutrino-nucleus reaction cross sections for a representative case of the ν - ^{12}C scattering. For the incident neutrino energy we take $E_\nu = 1$ GeV, a value lying in the energy region of current importance for many neutrino oscillation experiments. We first discuss the pion-production cross sections, which are our main results, and subsequently we consider the combined contributions of the pion-production and quasi-elastic processes.

The differential cross sections for the $\nu_e^{12}\text{C} \rightarrow e^- \pi X$ reaction, normalized with the target mass number ($A = 12$), are shown in Fig. 3, for the lepton scattering angle $\theta = 10^\circ$ and 30° , as a function of the invariant mass $W = \sqrt{-Q^2 + m_N^2 + 2\omega m_N}$. The dashed curve is the cross section obtained simply by taking the average of the incoherent contributions of the free protons and neutrons, while the Fermi-gas model results are shown by the dash-double-dotted curves. As expected, the inclusion of the nucleon Fermi motion widens the resonance width compared with the free nucleon case. The dash-dotted curves, corresponding to the case that includes the Pauli blocking effect for the final nucleon, indicate that the blocking effect reduces the forward cross section by about 20%. As mentioned in connection to Eq. (8), the inclusion of the Pauli blocking effect for the π -production process requires the knowledge of the pion-production amplitude. This implies that this effect cannot be evaluated by taking (as often done in the literature) the incoherent sum of the free-nucleon pion-production strength over the Fermi sea. (The role of Pauli blocking, however, diminishes for larger angles, where the momentum transfer becomes larger than the Fermi momentum.) The solid curves show the results of our full calculation that includes the spectral function taken from Ref. [29]; it is seen that the nuclear correlation effects further broaden the peak width and reduce the peak height by about 20%.

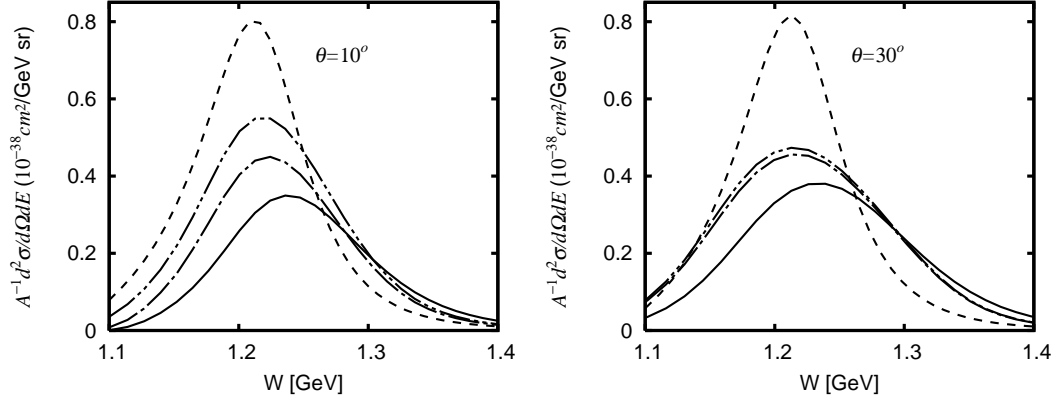


Fig. 3. Differential cross sections for $\nu_e^{12}\text{C} \rightarrow e^- \pi X$ at $\theta = 10^\circ$ and 30° . Dashed line – free-nucleon; dashed-double-dotted line – Fermi-gas model; dashed-dotted line – Fermi-gas model with Pauli blocking; solid line – full calculation.

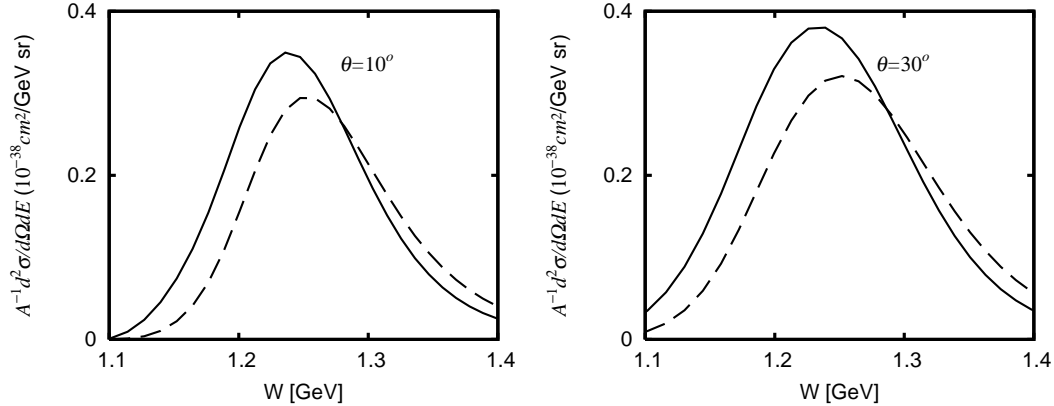


Fig. 4. Differential cross sections for $\nu_e^{12}\text{C} \rightarrow e^- \pi X$ at $\theta = 10^\circ$ and 30° . The dashed line represents the case where the pion production amplitude contains the dressed Δ contribution alone, while the solid line shows the results of our full calculation.

As discussed, the non-resonant mechanism contained in the SL-model plays a more pronounced role for the neutron than for the proton. To illustrate how this feature affects the neutrino-nucleus reaction, we give in Fig. 4 the differential cross sections for $\nu_e^{12}\text{C} \rightarrow e^- \pi X$ calculated with and without the non-resonant contributions; the solid curve is the result of the full calculation, while the dashed curve presents the case where only the contribution of the dressed resonance amplitude is considered. As expected, the resonance-only approach underestimates the cross sections by about 20% even in the resonance region. The full calculation is found to give more strength for lower values of W than the resonance-only case.

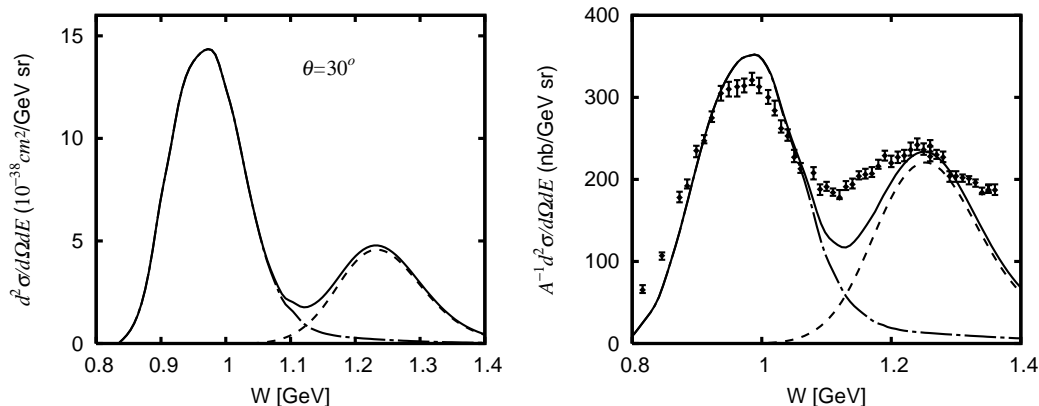


Fig. 5. Left panel – Differential cross section for the $\nu_e^{12}\text{C} \rightarrow e^- X$ reaction at $E_\nu = 1$ GeV and $\theta = 30^\circ$. Right panel – Differential cross section for the $e^- + ^{12}\text{C} \rightarrow e^- X$ reaction at $E_e = 1.1$ GeV with $\theta_e = 37.5^\circ$. The experimental data points are from Ref. [30].

To the contribution of the pion-production process we now add the contribution of the quasi-free nucleon knockout process. The latter is calculated using again the modified Fermi-gas model that incorporates the spectral function [7,29]. At the incident energy under consideration, the sum of these two contributions is expected to give the bulk of the inclusive reaction cross section. The differential cross section for $\nu_e^{12}\text{C} \rightarrow e^- X$ at $\theta = 30^\circ$ is shown in the left panel in Fig. 5. The bump at the lower energy is due to quasi-free nucleon knockout, while the higher energy bump is due to Δ -resonance excitation. To examine the validity of our present approach, we apply the same calculational framework to the $e^- + ^{12}\text{C} \rightarrow e^- X$ reaction (with the weak current replaced by the electromagnetic current), and compare the results with the experimental data. Fig. 5 shows this comparison. It is seen that the general trend of the data is reproduced reasonably well; in particular, the magnitude of the cross section in the Δ -resonance region is well reproduced. We remark that a calculation by Benhar *et al.* [7](BFNSS) underestimates the height of the Δ peak. According to Ref. [31], this is perhaps mainly due to the fact that, around the Δ region, the neutron structure functions of Ref. [32] used in BFNSS are significantly weaker than those extracted from an analysis of inclusive electron scattering on the deuteron. It is noteworthy that the SL model, in addition to providing a satisfactory description of the proton structure functions [20], gives neutron structure functions that are in good agreement with those deduced in Ref. [31]; see Fig. 6. This feature explains the difference in the Δ peak height between our results and those of BFNSS.

We note, however, that our calculation gives a dip structure that is somewhat too deep, a feature that seems to indicate that we need to go beyond ‘impulse’

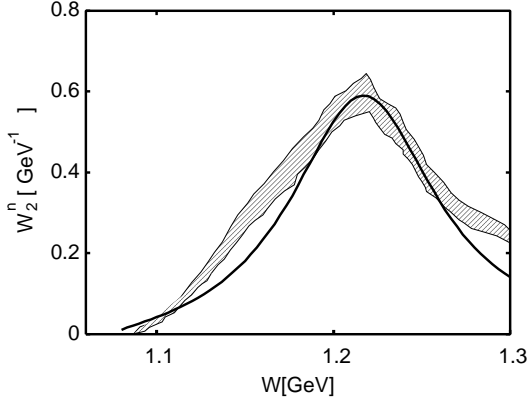


Fig. 6. The neutron structure function W_2^n at $E_e = 2.445\text{GeV}$ and $\theta_e = 20^\circ$. The solid line represents the results of the SL-model and the shaded area represents the W_2^n from the analysis of Ref. [31].

approximation and/or employ more elaborate treatments of nuclear correlation effects; see also Ref. [9]. It is also to be noted that in the higher W region our model, which only includes the Δ -resonance, is likely to underestimate the transition strength.

For some purposes it seems useful to present our results in the form of Q^2 -distribution [$Q^2 = -(p_\nu - p_l)^2$] or E_l -distribution. We get $d\sigma/dQ^2$ and $d\sigma/dE_l$ using the formulas,

$$\frac{d\sigma}{dQ^2} = \int dE_l \frac{\pi}{p_\nu p_l} \frac{d\sigma}{d\Omega_l dE_l}, \quad \frac{d\sigma}{dE_l} = \int d\Omega_l \frac{d\sigma}{d\Omega_l dE_l}. \quad (11)$$

Fig. 7 gives the Q^2 and E_μ spectra for the $\nu_\mu^{12}\text{C}$ reaction at $E_\nu = 1\text{ GeV}$; the left (right) panel corresponds to the CC (NC) reaction. The total contribution (solid line) consists of the quasi-free contribution (dash-dotted line) and the pion production contribution (short-dashed line). We note that the pion production contribution is reduced by the introduction of the spectral function. Finally, the muon energy distribution $d\sigma/dE_\mu$ in the $\nu_\mu^{12}\text{C} \rightarrow \mu^- X$ reaction is shown in Fig. 8.

5 Summary

We have studied the neutrino-nucleus and electron-nucleus reactions in the Δ -resonance region with the use of the Sato-Lee (SL) model, which allows us to treat the resonant and non-resonant contributions in a unified manner in deriving the amplitudes for pion electroweak production on a nucleon. The validity of SL has been extensively tested for electromagnetic observables involving single-nucleon targets, and we can use the available electron-nucleus

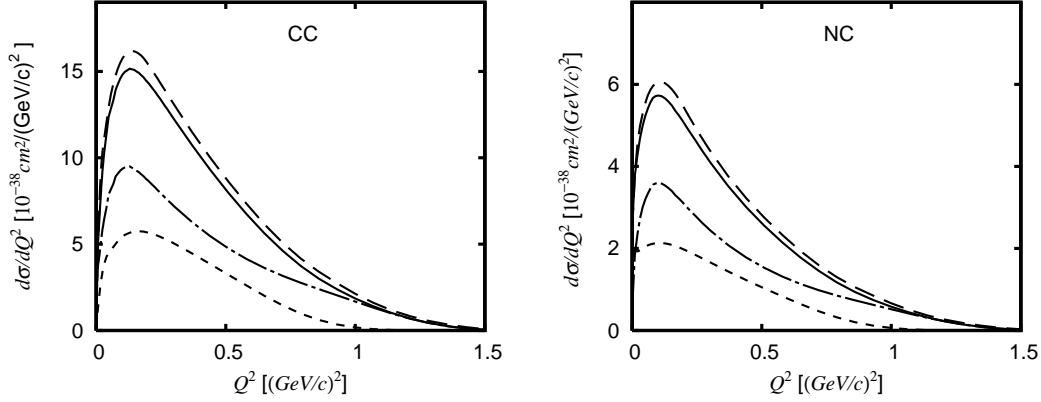


Fig. 7. The differential cross section $d\sigma/dQ^2$ for $\nu_\mu^{12}\text{C} \rightarrow \mu^- X$ and $\nu^{12}\text{C} \rightarrow \nu X$ at $E_\nu = 1$ GeV. The sum of the quasi-free and pion-production contributions is shown by the solid line (full calculation), and by the long-dashed line (Fermi-gas model). The individual contribution of the quasi-free process is shown by the dash-dotted line, and that of the pion-production process by the short-dashed line.

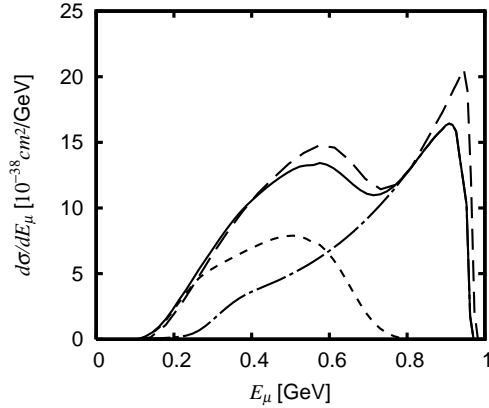


Fig. 8. Muon energy distribution $d\sigma/dE_\mu$ for the $\nu_\mu^{12}\text{C} \rightarrow \mu^- X$ reaction. The contributions of the quasi-free and pion-production reactions are shown in the short-dashed and dash-dotted lines, respectively, while their sum is given by the solid line. The long-dashed line represents the results obtained in the Fermi-gas model.

scattering data to assess the reliability of the application of SL to neutrino-nucleus reactions. As for the nuclear correlation effects, we have considered here only those effects which can be considered to be subsumed in the spectral function. Despite this rather limited treatment of the nuclear effects, our calculation based on SL gives reasonably good descriptions of the relevant electron scattering data; the peak structure in the cross section in the resonance region is well reproduced by our calculation. It is reasonable to expect that

our calculation of the neutrino-nucleus reaction cross sections based on the SL model enjoys the same level of success. It seems worthwhile to further develop SL studies of neutrino- and electron-nucleus reactions by elaborating the treatment of the nuclear effects (including medium effects on the Δ -resonance itself).

Acknowledgments

The authors are grateful to M. Sakuda for useful discussions. This work is supported by the U.S. National Science Foundation, Grant No. PHY-0457014, by the Japan Society for the Promotion of Science Grant-in-Aid for Scientific Research(c) 15540275, and by the U.S. Department of Energy, Nuclear Physics Division Contract No. DE-AC02-06CH11357.

References

- [1] J.G. Morfin, M. Sakuda and Y. Suzuki (eds), Proceedings of the First International Workshop on Neutrino-Nucleus Interactions in the Few GeV Region (NuInt01), Nucl. Phys. B (Proc. Suppl.) 112 (2002).
- [2] H. Tanaka and the K2K Collaboration, Nucl. Phys. B (Proc. Suppl.) 159 (2006) 38.
- [3] M.O. Wascko and the MiniBooNE Collaboration, Nucl. Phys. B (Proc. Suppl.) 159 (2006) 50.
- [4] R. Petti, Nucl. Phys. B (Proc. Suppl.) 159 (2006) 56.
- [5] A. Belias and the MINOS Collaboration, Nucl. Phys. B (Proc. Suppl.) 159 (2006) 63.
- [6] E. Kolbe, K. Langanke, G. Martinez-Pinedo and P. Vogel, J. Phys. G 29 (2003) 25.
- [7] O. Benhar, N. Farina, H. Nakamura, M. Sakuda and R. Seki, Phys. Rev. D 72 (2005) 053005.
- [8] S. K. Singh, M. J. Vicente Vacas and E. Oset, Phys. Lett. B 416 (1998) 23; erratum-ibid. B 423 (1998) 428; J. Nieves, J.E. Amaro, M. Valverde, Phys. Rev. C 70 (2004) 055503; erratum-ibid. C 72 (2005) 019902; J. Nieves, M. Valverde and M. J. Vicente Vacas, Phys. Rev. C 73 (2006) 025504.
- [9] A. Gil, J. Nieves and E. Oset, Nucl. Phys. A 627 (1997) 543; J. Nieves, J. E. Amaro, M. Valverde and E. Oset, nucl-th/0503023.

- [10] T. Sato, B. Szczerbinska, K. Kubodera and T.-S.H. Lee, Nucl. Phys. B (Proc. Suppl.) 159, (2006) 141; nucl-th/0601069.
- [11] T. Leitner, L. Alvarez-Ruso and U. Mosel, Phys. Rev. C 73 (2006) 065502.
- [12] R. A. Smith and E. J. Moniz, Nucl. Phys. B 43 (1972) 605.
- [13] T. Kuramoto, M. Fukugita, Y. Kohyama and K. Kubodera, Nucl. Phys. A 512 (1990) 711.
- [14] D. Rein and L.M. Sehgal, Ann. Phys. 133 (1981) 79.
- [15] O. Lalakulich and E. A. Paschos, Phys. Rev. D 71 (2005) 074003.
- [16] O. Lalakulich, E.A. Paschos and G. Piranishvili, Phys. Rev. D 74 (2006) 014009.
- [17] T. Sato and T.-S. H. Lee, Phys. Rev. C 54 (1996) 2660.
- [18] T. Sato and T.-S. H. Lee, Phys. Rev. C 63 (2001) 055201.
- [19] T. Sato, D. Uno and T.-S. H. Lee, Phys. Rev. C 67 (2003) 065201.
- [20] K. Matsui, T. Sato and T. -S. H. Lee, Phys. Rev. C 72 (2005) 025204.
- [21] T.R. Hemmert, B.R. Holstein and N.C. Mukhopadhyay, Phys. Rev. D 51 (1995) 158; J. Liu, N.C. Mukhopadhyay and L. Zhang, Phys. Rev. C 52 (1995) 1630.
- [22] T. Kitagaki *et al.*, Phys. Rev. D, 42 (1990) 1331.
- [23] V. V. Frolov et al., Phys. Rev. Lett 82 (1999) 45.
- [24] K. Joo et al., Phys. Rev. Lett. 88 (2002) 122001.
- [25] Y. Horikawa, F. Lenz and N.C. Mukhopadhyay, Phys. Rev. C 22 (1980) 1680.
- [26] M. C. Martinez, P. Lava, N. Jachowicz, J. Ryckebusch and K. Vantournhout, Phys. Rev. C 73 (2006) 024607.
- [27] J. H. Koch and N. Ohtsuka, Nucl. Phys. A 435 (1985) 765. M. Hirata, F. Lenz and K. Yazaki, Ann. Phys. 108 (1977) 116.
- [28] W. Cassing, M. Kant, K. Langanke and P. Vogel, Phys. Lett. B 639 (2006) 32.
- [29] O. Benhar, A. Fabrocini, S. Fantoni and I. Sick, Nucl. Phys. A 579 (1994) 493.
- [30] R. M. Sealock et al., Phys. Rev. Lett. 62 (1989) 1350.
- [31] O. Benhar and D. Meloni, Phys. Rev. Lett 97 (2006) 192301.
- [32] A. Bodek and J. L. Ritchie, Phys. Rev. D 23 (1981) 1070.